POLITECNICO
MILANO 1863

SCUOLA DI INGEGNERIA INDUSTRIALE
E DELL'INFORMAZIONE

Executive Summary of the Thesis

Station keeping of Halo orbits at the Sun-Earth and Earth-Moon L2: failure analysis with the Floquet mode approach

Laurea Magistrale in Space Engineering - Ingegneria Spaziale

Author: Davide Intravaia

Advisor: Prof. Camilla Colombo

Co-advisors: Elisa Maria Alessi, Mathilda Bolis

Academic year: 2022-2023

1. Introduction

In the context of the Circular Restricted Three Body Problem (CR3BP), interest in space missions around Lagrange points has grown in recent years for both the Sun-Earth and Earth-Moon systems. Most of these missions are take place around Lagrange Points L_1 and L_2 [12]. These are unstable locations, thus a spacecraft (s/c), located on an operational orbit in their vicinity, requires station keeping. Many station keeping algorithms have been developed through the years [12]. One of this is the Floquet Mode Approach (FMA) [13].

In this thesis the FMA has been developed and deeply studied to understand its application limits in the case of Halo orbits around Sun-(Earth+Moon) and Earth-Moon L_2. This study, through the use of a Monte Carlo simulation, investigates in which cases the control algorithm fails, with respect to two parameters: the minimum time between maneuvers and the amplitude of Halo orbits.

Furthermore, within the established operational limits, this study includes two distinct applications. The former concerns the Radiation Environment Monitor for Energetic Cosmic rays (REMEC) mission. In this case, a preliminary analysis is performed to assess station keeping costs. The second application involves the Bi-Circular Restricted Four Body Problem (BR4BP), where the algorithm's utility is explored in a different dynamical model.

2. Circular Restricted Three Body Problem

The thesis is mainly developed in the CR3BP dynamics. Graphically represented Fig. 1.

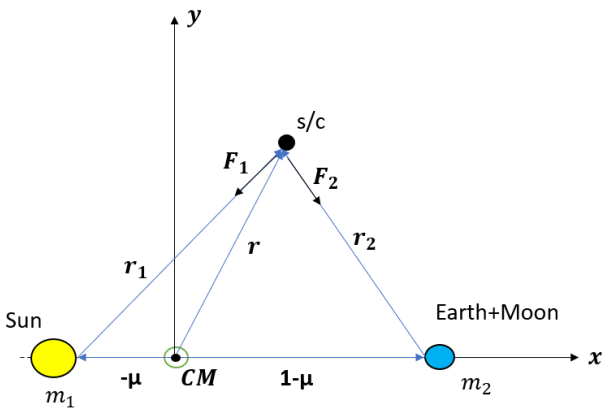

Figure 1: Schematic representation of CR3BP.

Using the notation expresses in Fig. 1, the dimensionless equations of motion [2, 16] in

CR3BP are expressed as Eq. (1).

$$\begin{cases} \ddot{x} - 2\dot{y} = V_x, \\ \ddot{y} + 2\dot{x} = V_y, \\ \ddot{z} = V_z. \end{cases} \tag{1}$$

Where V_x, V_y and V_z are the partial derivatives of the total potential (Eq. (4)):

$$\begin{cases} V_x = x - \dfrac{1-\mu}{r_1^3}(x+\mu) - \dfrac{x+\mu-1}{r_2^3}\mu, \\ V_y = y - \dfrac{1-\mu}{r_1^3}y - \dfrac{\mu}{r_2^3}y, \\ V_z = -\dfrac{1-\mu}{r_1^3}z - \dfrac{\mu}{r_2^3}z. \end{cases} \tag{2}$$

Where,

$$\begin{cases} r_1 = \sqrt{(x+\mu)^2 + y^2 + z^2}, \\ r_2 = \sqrt{(x+\mu-1)^2 + y^2 + z^2}. \end{cases} \tag{3}$$

In this form, the equations of motion depend only on the mass parameter μ.

$$V = \frac{1}{2}(x^2 + y^2) + \frac{1-\mu}{r_1} + \frac{\mu}{r_2} \tag{4}$$

2.1. Halo orbits

Halo orbits are 3D periodic and symmetric with respect to $x - z$ plane. They can be computed analytically, considering the in-plane and out-of-plane frequencies to be equal [4]. In this thesis, Halo orbits are computed numerically. A differential correction technique that exploits the orbits' symmetry and the State Transition Matrix (STM) to adjust the initial conditions and find the correct ones. For the purpose of this thesis, it is important to know that when the amplitude A_z increases, Halo orbits become more stable: stability index decreases.

2.2. Monodromy matrix

The Monodormy matrix $\boldsymbol{M}$ corresponds to the STM evaluated after one orbital period. The eigenvalues of $\boldsymbol{M}$ provide information on the global stability of Halo orbits: $m_1 > 1$ and $m_2 = 1/m_1 < 1$ represent the unstable and stable components, while $m_3 = m_4$ and $m_5 = m_6^{*1}$ lie on the unit circle that represents marginal stability. Moreover, eigenvectors associated with m_1 and m_2 represent stable and unstable direction of the hyperbolic manifolds towards and from the periodic orbit.

[1] * means complex and conjugate eigenvalues

3. Floquet Mode Approach

FMA is a control method used in the CR3BP framework, that makes use of the theory of invariant manifolds. The method, developed in [6, 13], aims to cancel the unstable component of the error state vector, such that the s/c can naturally converge towards the nominal orbit. The information about stable and unstable directions are not recovered from STM, since its elements grow exponentially in time, but from the Floquèt modes.

3.1. Floquet Modes

Floquet modes can be computed numerically following procedure in [9], with the following formula:

$$\tilde{\boldsymbol{E}}(t, t_0) = \boldsymbol{\Phi}(t, t_0) S e^{-\tilde{\boldsymbol{J}}t} \tag{5}$$

Where matrix $\boldsymbol{S}$ is a real matrix that collects the eigenvectors of $\boldsymbol{M}$, $\tilde{\boldsymbol{J}}$ is a Jordan matrix that depends on the eigenvalues of $\boldsymbol{M}$ and $\boldsymbol{\Phi}(t, t_0)$ is the STM at the given time.

3.2. Controller definition

Different controllers based on the FMA exist [5, 8, 9], but the aim of all of them is to eliminate the unstable component of the error state vector. In this work, a one-axis controller Eq. (6) and a two-axes controller Eq. (7) are implemented.

$$\Delta_x = -\frac{c_1}{\pi_4} \tag{6}$$

$$\Delta_x = -\frac{c_1 \pi_4}{\pi_4^2 + \pi_5^2(t)} \quad ; \Delta_y = -\frac{c_1 \pi_5}{\pi_4^2 + \pi_5^2} \tag{7}$$

Where $\boldsymbol{\pi}_1 = [\pi_1; \pi_2; \pi_3; \pi_4; \pi_5; \pi_6]$ is the projection factor along the unstable direction and $c_1 = \boldsymbol{\pi}_1(t) \cdot \boldsymbol{\delta}(t)$ is the unstable component, with $\boldsymbol{\delta}(t) = [\delta x \ ; \delta y \ ; \delta z \ ; \delta \dot{x} \ ; \delta \dot{y} \ ; \delta \dot{z}]$ the error state vector, the difference between the actual spacecraft position and the nominal orbit.

4. Simulation

As already mentioned, a Monte Carlo simulation, with 100 trials [7], is performed varying two parameters: minimum time between two consecutive maneuvers, Δt_{min}, and Halo amplitude along the z direction, A_z.
In this simulation a maneuver is performed when

the deviation with respect to the nominal orbit overcomes a certain limit. Two boundaries have been defined: *Starting maneuver* and *Limit maneuver*. Maneuvers are not executed below the *Starting maneuver* boundary, but within the range defined by the *Starting maneuver* and *Limit maneuver* boundaries. Indeed, a maneuver is executed if the s/c deviates from the nominal orbit, while if the s/c exceeds the *Limit maneuver* boundary, the station keeping is considered to have failed.
Furthermore, orbit determination (OD) errors, orbit injection (OI) errors and magnitude maneuver errors are included in the simulation, to make it more realistic.
The simulation has been conducted for both the Sun-(Earth+Moon) and Earth-Moon systems. However, as the same conclusions can be drawn for both systems, only the results for the Sun-(Earth+Moon) case will be presented herein.

4.1. Sun-(Earth+Moon)

The orbits considered for Sun-(Earth+Moon) case are listed in Table 1.

A_z [km]	T [days]	k
$6.27 \cdot 10^3$	180.38	1695
$3.62 \cdot 10^5$	180.04	1458.13
$6.95 \cdot 10^5$	179.02	978.13
$9.94 \cdot 10^5$	177.16	548.75
$1.38 \cdot 10^6$	171.57	174.67
$1.65 \cdot 10^6$	161.06	45.68
$1.72 \cdot 10^6$	155.21	24.81
$1.77 \cdot 10^6$	149.84	14.24
$1.80 \cdot 10^6$	144.61	7.93
$1.82 \cdot 10^6$	139.42	3.89

Table 1: Amplitudes, periods and stability indexes of the selected orbits for Sun-(Earth+Moon) system.

In Table 2 the input parameters are defined.
Figure 2 shows the success probability of the station keeping algorithm implemented with the FMA, as function of the Δt_{min} and A_z.

Input parameters	
Number of orbits	10
OD errors	1.5 km and 1 cm/s
OI errors	150 km and 3 cm/s
Maneuver errors	5% in magnitude
Tracking points	one per day
Starting maneuver	500 km
Limit maneuver	50000 km
MC trials	100
$\boldsymbol{\mu}$	$3.04042 \cdot 10^{-6}$ [15]

Table 2: Input parameters for Monte Carlo simulation in the Sun-(Earth+Moon) system

The first interesting observation that can be done is that the two-axis controller (Fig. 2b) provides an overall greater number of successes with respect to one-axis controller (Fig. 2a): in particular higher amplitudes are better controlled. For both cases two common behaviours have been identified:

1. Increasing Δt_{min} the station keeping starts to fail.
2. Increasing the amplitudes A_z, even if Δt_{min} is low, the station keeping fails.

Increasing Δt_{min} limits station-keeping effectiveness as it constrains to control less the orbit, eventually leading to failure. Halo orbits become more stable with higher A_z values, suggesting that station-keeping failing with a low amplitude orbit at a specific Δt_{min} might succeed with the same Δt_{min} but a larger amplitude orbit. The second behavior is due to the Floquet mode approach's structure. Instead, if the stable component is weak, the s/c can't converge to the nominal orbit, as the method cancel the error state vector along the unstable component. Remember that, system stability depends on eigenvalues within the unit circle on the complex plane. In Fig. 3, two zones are distinguishable: success and failure zones. In the success zone, the strong stable component keeps the spacecraft on a nominal orbit when cancelling the unstable one. In the failure zone, the weakening stable component can't maintain s/c bounded. Between the two zones, there is a transition region where the station keeping could succeed or not.

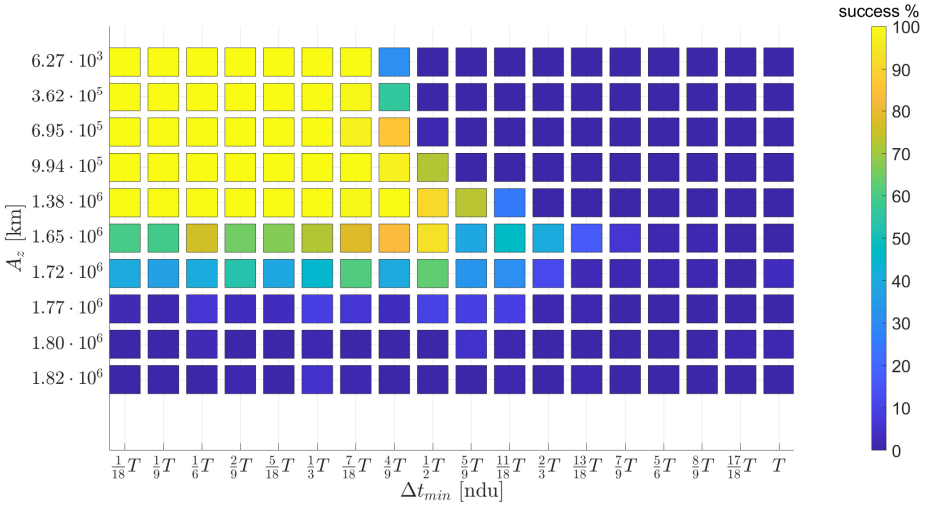

(a) One-axis controller

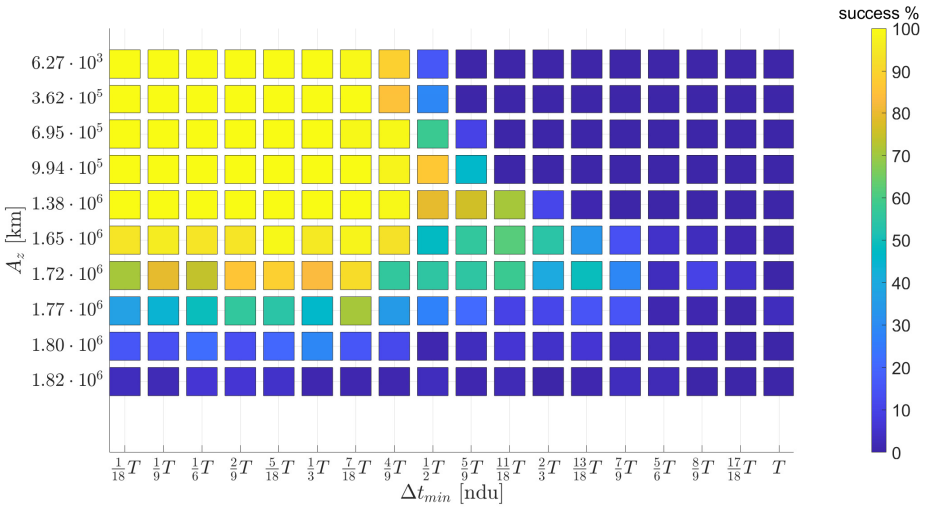

(b) Two-axis controller

Figure 2: Successes of Floquet mode approach: Halo orbits around L_2 in Sun-Earth system.

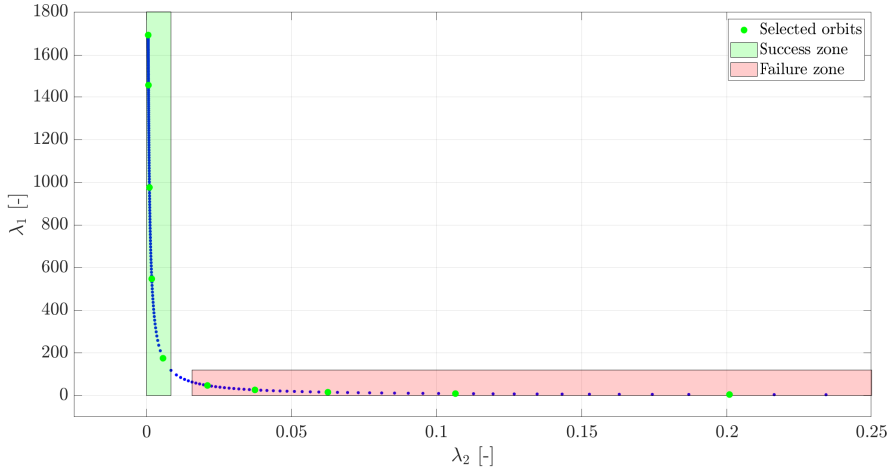

Figure 3: Unstable and stable eigenvalues of Halo orbits around L2 in Sun-(Earth+Moon) system.

5. Application

Within the defined operational limits, two applications of the algorithm will be presented: one referring to the baseline operational orbit of the REMEC mission [1], and one with the same orbit defined in the BR4BP.

5.1. Application A: REMEC

The operational orbit of the baseline mission [10] has an amplitude $A_z = 280000$ km. The aim of the analysis was to make a preliminary definition of station keeping costs. Also in this case, a Monte Carlo simulation is performed to obtain more significant results. The input parameters for the simulation are listed in Table 3.

Input parameters	
Number of orbits	10
OD errors	1.5 km and 1 cm/s
OI errors	150 km and 3 cm/s
Maneuver errors	5% in magnitude
$\boldsymbol{\Delta t_{min}}$	30 days
Tracking points	one per day
Starting maneuver	500 km
Limit maneuver	50000 km
MC trials	100
$\boldsymbol{\mu}$	$3.04042 \cdot 10^{-6}$ [15]

Table 3: Input parameters for the station keeping algorithm for REMEC mission

Two simulations were done: with and without Solar Radiation Pressure (SRP). The cannonball model [14] has been implemented. The acceleration term, Eq. (8), is added to the left hand side of Eq. (1).

$$a_s = \frac{P_{SC} A_{SC}}{m_{SC}} \rho_r \tag{8}$$

Where the mass of the s/c is $m_{SC} = 100\ kg$, the surface area hit by the Sun is $A_{SC} = 1.570604\ m^2$ and the reflectivity coefficient $\rho_r = 1.8$.
Table 4 and Table 5 show the results of the simulation. It is evident that with the presence of SRP, the performances are worst. The SRP acts continuing pushing the s/c.

	Mean	**STD**
Error	612.15 km	89.60 km
SK cost	4.04 m/s	1.01 m/s
n° of maneuver	33	3

Table 4: Simulation results REMEC mission (no SRP).

	Mean	**STD**
Error	8550.39 km	1112.63 km
SK cost	69.55 m/s	5.11 m/s
n° of maneuver	44	1

Table 5: Simulation results REMEC mission (with SRP).

5.2. Application: BR4BP

An application has been analyzed in the B4BP. The dynamics is modified as in [11]. In this case, the Moon is included inside the dynamics as a perturbation, thus the total potential, Eq. (4), becomes:

$$V_M(x, y, z, \mu, \theta) = V(x, y, z, \mu, \theta) + \frac{m_M}{r_M} - \frac{m_M}{\rho_M^2}(x \cos\theta + y \sin\theta) \tag{9}$$

Where $\dot{\theta} = \omega_M = 12.367\ [ndu]$ is the Moon mean angular velocity with respect to Earth, $m_M = 3.6942 \cdot 10^{-8}\ [ndu]$ is the Moon mass, $\rho_M = 2.5721 \cdot 10^{-3}\ [ndu]$ is the mean Earth-Moon distance and $r_M^2 = (x-1+\mu-\rho_M \cos\theta)^2 + (y - \rho_M \sin\theta)^2$ is the s/c-Moon distance.
The aim was to apply the station keeping algorithm in this new dynamics, to represent a more realistic scenario. Using the same input parameters reported in Table 3, with the only difference in *Limit maneuver*=500000 km, the results are reported in Table 6.

	Mean	**STD**
Error	124934.33 km	7472.16 km
SK cost	2210.51 m/s	266.89 m/s
n° of maneuver	49	1

Table 6: Simulation results in BR4BP.

The results, in particular the SK cost, are worse than in the CR3BP case, but were predictable as the Moon is introduced as a perturbation and therefore the station keeping algorithm has to compensate for it. Moreover, the initial conditions, for the Halo orbit propagation, are found in CR3BP thus they don't exist in BR4BP. However, the input parameters can be changed as shown in Table 7.

Input parameters	
Number of orbits	1
OD errors	0
OI errors	0
Maneuver errors	0
$\boldsymbol{\Delta t_{min}}$	1 days
Tracking points	one per day
Starting maneuver	100 km
Limit maneuver	50000 km
MC trials	100
$\boldsymbol{\mu}$	$3.04042 \cdot 10^{-6}$ [15]

Table 7: Input parameters to compute a reference orbit in BR4BP

In this way, the mean error is equal to 12299.15 km. The graphical representation of the simulation is shown in Fig. 4. Since the orbit in this way is controlled, it is assumed that it is possible to use it as initial guess for future refinement in a more realistic dynamics.

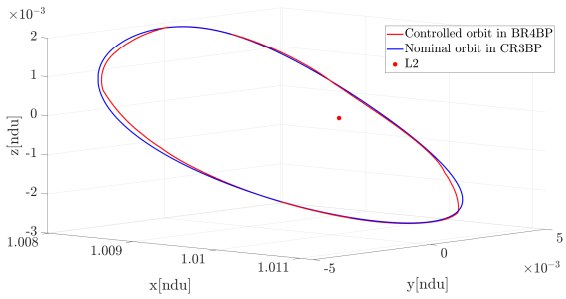

Figure 4: Controlled orbit in BR4BP to use as initial guess for future refinement.

6. Conclusions

In this work, the limits of the FMA are shown. Since FMA exploits stable component to keep the s/c bounded around the nominal orbits, Halo orbits with a small unstable component, and therefore a larger stable component, are more difficult to control than orbits with a higher unstable component. In addition, the FMA was implemented varying the minimum time between maneuvers Δt_{min} and amplitude A_z of the Halo orbits, to see how the algorithm was influenced by these parameters. As a general consideration, performances can be improved implementing a two-axes controller: Δt_{min} and A_z can be grater.
Within the identified operating limits, two applications were made. Application A: the results of the station keeping are in in agreement with literature [3, 5, 6, 12, 13]. Application B: station keeping was tested inside the BR4BP to verify if it was able to control a s/c. It turned out that the FMA was able to keep a s/c bounded around a nominal orbit, even if the station keeping costs are not reasonable.

6.1. Future works

As just said, FMA has some limitations, specifically respect to orbits with a very little unstable component. For this reason, it is suggested to perform the same analysis as described in Section 4, implementing another method, such as Hamiltonian Structure Preserving to check whether this method is able to control all orbits of the Halo family.
Moreover, since an orbit in BR4BP has been computed using the FMA, this orbit could be used as initial guess for future refinement of the same orbit but in the four-body dynamics.

References

[1] A. Aguilar, R. Filgas, C. Colombo, E. M. Alessi, M. lo Iacono, E. Arikan, and M. Bolis. The remec mission: Mission concept and architecture feasibility assessment. Technical report, 2023.

[2] G. Colasurdo and G. Avanzini. Astrodynamics. *Ch*, 6:88–90, 2006.

[3] S. Cravedi. Floquet modes approach. Master's thesis, Politecnico di Milano, 2019. Supervisor: Prof. Francesco Topputo.

[4] R. W. Farquhar and A. A. Kamel. Quasi-periodic orbits about the translunar libration point. *Celestial Mechanics and Dynamical Astronomy*, 1973.

[5] A. Farrès, G. Gòmez, J. Masdemont, C. Webster, and D. C. Folta. In *The Geometry of Station-Keeping Strategies around Libration Point Orbits*. 70th International Astronautical Congress, IAF, 2019.

[6] G. Gomez, J. Llibre, R. Martinez, and C. Simò. *Dynamics and Mission Design Near Libration points*. World Scientific Publishing Co. Pte. Ltd., 2001.

[7] S. C. Gordon. *Orbit determination erro and analysis and station-keeping for libration point trajectories*. PhD thesis, Purdue University, West Lafayette, Indiana, 1991.

[8] G. Gòmez, K. Howell, J. Masdemont, and C. Simò. Station-keeping strategies for translunar libration ppoint orbits. *Advances in the Astronautical Sciences*, 1998.

[9] T.M. Keeter. Station-keeping strategies for libration point orbits: Target point and floquet mode approaches. Master's thesis, Purdue University, West Lafayette, Indiana, 1994.

[10] M. Lo Iacono. Parametric design for earth to sun-earth l2 halo transfers in the circular restricted three body problem. Master's thesis, Politecnico di Milano, 2023. Supervisor: Prof. Camilla Colombo.

[11] G. Mingotti and F. Topputo. Ways to the moon: A survey. *Advances in the Astronautical Sciences*, 2011.

[12] M Shirobokov, S Trofimov, and M Ovchinnikov. Survey of station-keeping techniques for libration point orbits. *Journal of Guidance, Control, ans Dynamics*, 2017.

[13] C Simò, G Gomez, J Llibre, R Martinez, and J Rodriguez. On the optimal station keeping control of halo orbits. *Acta Astronautica*, pages 391–397, 1987.

[14] S. Soldini. *Design and Control of Solar Radiation Pressure Assisted Missions in the Sun-Earth Restricted Three-Body Problem*. PhD thesis, University of Southampton, 2016.

[15] M. Stramacchia, C. Colombo, and F. Bernelli-Zazzera. Distant retrograde orbits for space-based near earth objects detection. *Advances in Space Research*, pages 967–988, 2016.

[16] V. Szebehely. *Theory of orbits in the restricted problem of three bodies*. Press Inc., New York., 1967.